Neurobiology of Disease 132 (2019) 104602

Contents lists available at ScienceDirect

Neurobiology of Disease

journal homepage: www.elsevier.com/locate/ynbdi

Purkinje cell-specific *Grip1/2* knockout mice show increased repetitive self-grooming and enhanced mGluR5 signaling in cerebellum

Rebeca Mejias[a,c,**], Shu-Ling Chiu[b], Mei Han[a], Rebecca Rose[a], Ana Gil-Infante[c], Yifan Zhao[a], Richard L. Huganir[b], Tao Wang[a,*]

[a] McKusick-Nathans Department of Genetic Medicine and Department of Pediatrics, Johns Hopkins University, Baltimore, MD 21205, USA
[b] Department of Neuroscience, Johns Hopkins University, Baltimore, MD 21205, USA
[c] Department of Physiology, University of Seville, 41012 Seville, Spain

ARTICLE INFO

Keywords:
Autism
Grooming
Cerebellum
Purkinje cells
Glutamate signaling
AMPA receptors
mGluR receptors
Grip1/2
LTD

ABSTRACT

Cerebellar Purkinje cell (PC) loss is a consistent pathological finding in autism. However, neural mechanisms of PC-dysfunction in autism remain poorly characterized. Glutamate receptor interacting proteins 1/2 (Grip1/2) regulate AMPA receptor (AMPAR) trafficking and synaptic strength. To evaluate role of PC-AMPAR signaling in autism, we produced PC-specific *Grip1/2* knockout mice by crossing *Grip2* conventional and *Grip1* conditional KO with L7-Cre driver mice. PCs in the mutant mice showed normal morphology and number, and a lack of Grip1/2 expression. Rodent behavioral testing identified normal ambulation, anxiety, social interaction, and an increase in repetitive self-grooming. Electrophysiology studies revealed normal mEPSCs but an impaired mGluR-LTD at the Parallel Fiber-PC synapses. Immunoblots showed increased expression of mGluR5 and Arc, and enhanced phosphorylation of P38 and AKT in cerebellum of PC-specific *Grip1/2* knockout mice. Results indicate that loss of Grip1/2 in PCs contributes to increased repetitive self-grooming, a core autism behavior in mice. Results support a role of AMPAR trafficking defects in PCs and disturbances of mGluR5 signaling in cerebellum in the pathogenesis of repetitive behaviors.

1. Introduction

Cerebellar dysfunctions have been implicated in autism pathogenesis but the underlying mechanisms remain poorly understood (Becker and Stoodley, 2013). Acquired cerebellar lesions were shown to give rise to symptoms that resemble core autism features including flattening of affect, gaze aversion, social withdrawal, impaired executive function, speech and language defects, and stereotyped movements (Schmahmann and Sherman, 1998; Levisohn et al., 2000; Riva and Giorgi, 2000; Gottwald et al., 2004). It was speculated that these symptoms arise from dysfunction of the pathways connecting the cerebellum to prefrontal, limbic, and striatal regions of the brain (Schmahmann and Sherman, 1998). Patients with autism were found to have a significant increase in the total cerebellar volume from an age of 3 years old to adolescence (Courchesne et al., 2001; Aparks et al., 2002; Herbert et al., 2003; Palmen et al., 2004), and a substantial increase of white matter volume in cerebellum (Courchesne et al., 2001). Further, grey matter regions of cerebellar vermis are frequently reduced in size in patients with autism (Levitt et al., 1999; Carper and Courchesne, 2000; Kaufmann et al., 2003), and this feature appears autism-specific as similar changes were not found in either Fragile X or Down syndrome (Kaufmann et al., 2003).

Purkinje cell loss is the most consistent pathological finding in brains from autism patients (Bauman and Kemper, 1985, Ritvo et al., 1986, and review by Allen, 2005). The loss of PCs in autistic patients is associated with changes in key cerebellar proteins involved in apoptosis (Bcl2 and p53) (Araghi-Niknam and Fatemi, 2003), astroglial activation (GFAP) (Laurence and Fatemi, 2005), GABAergic signaling pathway (GAD65/67) (Fatemi et al., 2002), and glutamatergic synaptic functions (GluA1, EAAT1, and Grip1) (Purcell et al., 2001). Studies of mutant

Abbreviations: AMPAR, AMPA receptor; FMRP, Fragile X mental retardation protein; Grip1/2, glutamate receptor interacting proteins 1/2; LTD, Long-term potentiation; mEPSC, miniature excitatory synaptic current; L7, Let-7; MPEP, 2-methyl-6-phenylethynyl-pyridine; PC, Purkinje cell; TSC, Tuberous sclerosis; VPA, Valproic acid

* Corresponding author at: McKusick-Nathans Institute of Genetic Medicine and Department of Pediatrics, Johns Hopkins University School of Medicine, 733 North Broadway BRB 513, Baltimore, MD 21205, USA.
** Corresponding author at: Department of Physiology, School of Biology, University of Seville, Avenida de la Reina Mercedes s/n, 41012 Sevilla, Spain.
E-mail addresses: rmejias@us.es (R. Mejias), twang9@jhmi.edu (T. Wang).

https://doi.org/10.1016/j.nbd.2019.104602
Received 2 April 2019; Received in revised form 30 July 2019; Accepted 30 August 2019
Available online 30 August 2019

mice with Purkinje cell loss provide supporting evidence for a direct role of these cerebellar neurons in generating autism-related behaviors (Martin et al., 2010). PC-specific deletion of *Tsc1* or *Tsc2* results in PC loss and is sufficient to generate an autism-related phenotype, including increased repetitive grooming, deficits in sociability and abnormal ultrasonic vocalization(Reith et al., 2012; Tsai et al., 2012). Although these studies suggest a role of PCs and cerebellum in regulating repetitive behaviors such as repetitive self-grooming, the specific mechanims involved need further clarification. Self-grooming is an evolutionary conserved behavior involved in hygiene maintenance, social communication, and other important processes that is also observed in humans. Studies of rodent self-grooming could shed light in understanding the neural mechanisms involved in altered repetitive behaviors showed in certain neuropsychiatric disorders such as autism spectrum disorder and obsessive-compulsive disorder (reviewed by Kalueff et al., 2016).

Deficiency of FMRP (fragile X mental retardation protein) in cultured hippocampal neurons leads to an increase in internalization of AMPA receptor (AMPAR) GluA1, which is rescued by treatment with MPEP (2-methyl-6-phenylethynyl-pyridine), an mGluR5-specific inverse agonist (Nakamoto et al., 2007). *Fmr1*-KO mice show an exaggerated mGluR-dependent long-term depression (LTD) in hippocampus, probably associated with enhanced mGluR5 signaling, and exacerbated repetitive behaviors (Huber et al., 2002; McNaughton et al., 2008; Pietropaolo et al., 2011). In fact, antagonists of mGluR5 receptors can effectively reduce repetitive self-grooming behaviors in autism mouse models, such as BTBR mice (Silverman et al., 2010) and VPA (valproic acid)-treated mice (Mehta et al., 2011). In contrast, reduced mGluR-LTD and abnormal levels of Arc have been observed with *Tsc2* +/− and *Ube3A* KO mice that model for Tuberous Sclerosis 2 and Angelman Syndromes, respectively (Auerbach et al., 2011; Pignatelli et al., 2014). Taken together, these studies provide compelling evidences for a crucial link between mGluR-mediated signaling dysfunctions and cognitive and behavioral deficits in autism syndromes (Wilkerson et al., 2018).

Grip1/2 are neural scaffolding proteins that regulate AMPAR trafficking. Lack of neuronal specific *Grip1/2* expression results in deceleration of activity-dependent GluA2 recycling (Mao et al., 2010), lack of cerebellar LTD in cultured Purkinje-cells (Takamiya et al., 2008), and changes in social interactions in neuron-specific *Grip1/2* KO mice (Mejias et al., 2011). To dissect role of Grip1/2 in PCs with autism-related phenotypes, we generated PC-specific *Grip1/2* KO mice. These mice exhibited a significant increase in self-grooming but normal social interactions. Further studies revealed lack of mGluR-LTD at the Parallel Fiber-PC synapses and increased expression of mGluR5 signaling proteins in cerebellum. The results suggest a novel role for Grip1/2-mediated AMPAR recycling at cerebellar Purkinje cells in modulating self-grooming behaviors in mice.

2. Methods

2.1. Animals

PC-specific-*Grip1/2* knockout mice were generated by first breeding *Grip2* conventional KO mice with *Grip1* conditional (flox/flox) KO mice (Takamiya et al., 2008). Mice were then crossed to L7-Cre transgenic mice (Tsai et al., 2012). Heterozygous mice from this breeding were bred together to generate mice with the following two genotypes: (1) *Grip1*-flox/KO with *Grip2*-KO/KO (conventional KO) and L7-Cre positive heterozygous (L7-DKO), and (2) *Grip1/2* WT and L7-Cre-positive heterozygous (L7-control). L7-KO and L7-control mice are matched for mixed 129xC57BL/6 background. Genotype for L7-DKO and L7-control mice was determined by PCR screening using the following primers: 5′-AGA ATG GAC GCT TAC CTG CTC ATC C (RHKT 95), 5′-ATG CTC CAG ACT GCC TTG GGA AAA G (RHKT 83), and 5′-TAT CTG TCC CCT TCC GAT GCC CAT CTA C (RHKT 96) for Grip2 genotyping; 5′-TAA AGC CGC TGA GGA CGT TTG TGT CAC CTC (KT 196), 5′-CTA GTG AAC CTC TTC GAG GGA CCT AAT AAC (KT 198), 5′-ACA TTT TCC CTG GAC ACT TGG CGT TGA GCC (KT 199), and 5′-AAA AAT AGG CGT ATC ACG AGG C (84) for Grip1 genotyping; 5′- CAA TGT CTG ACC AAA TAC CAC CAC (KO 44) and 5′-TAA TCG CGA ACA TCT TCA GGT TCT GC (KO 42) for the L7-Cre transgene. For electrophysiological studies, *Grip2* conventional KO mice with neuron-specific deletion of *Grip1* (*Grip*-DKO, genotype: *Grip1*-flox/KO with *Grip2*-KO/KO and Nestin-Cre positive heterozygous) and *Grip2* conventional KO mice (*Grip*-SKO, genotype: *Grip1*-WT with *Grip2*-KO/KO) were obtained and genotyped as described before (Mao et al., 2010). Male L7-DKO, L7-control, Nestin-DKO and Nestin-control animals between 2 and 6 months of age were used in this study (n = 10–11 mice/ group). Mice were housed in temperature-controlled rooms with 12-h light/dark cycle (9:00 and 21:00) and had free access to water and standard mouse chow. Animal breeding and experimental procedures were conducted in strict accordance with the NIH Guide for Care and Use of Laboratory Animals. The study protocol was approved by the Animal Care and Use Committee at Johns Hopkins University.

2.2. Mouse behavioral testing

Mouse behavioral tests were conducted at the Animal Behavioral Core of the Johns Hopkins University School of Medicine following standard protocols from the Animal Behavioral Core User Manual (*http://www.brainscienceinstitute.org/index.php/cores*) (Pletnikov et al., 2008; Ayhan et al., 2011) and published protocols from our laboratories (Mejias et al., 2011; Adamczyk et al., 2012). The test order and age of the study cohorts of mice for individual test (in parenthesis) are as follow: open field and zero maze (2 month), self-grooming test, sociability and preference for social novelty (3 month), dyadic male-male interaction and rotarod (4 month), light and dark box (5 month). For individual test, L7-DKO and L7-control mice were always tested together to minimize variations. Test animals had at least one week break in between two tests. The average ambient lighting (lux) for individual behavioral test was described in previous publications (Mejias et al., 2011; Adamczyk et al., 2012).

2.2.1. Open-field test

Each individual test mouse was placed in a photo-beam (n = 16 at equal spacing of 2.5 cm) equipped clear plastic chamber (45 × 45 cm) and was allowed to explore free from interference for 30 min. The peripheral area (425 cm^2) was defined by the two side-photo beams, #1–2 and #15–16, while the central area (1600 cm^2) was defined by photo beams #3–14 at each direction. Movements in the chamber were tracked using a SDI Photobeam Activity System (San Diego Instruments). The patterns of ambulatory movement, fine movement, and rearing behavior at central and peripheral areas were automatically recorded and analyzed.

2.2.2. Zero maze

The zero maze for mice [51 cm (diameter, inside wall), 61 cm (diameter, outside wall), 61 cm (high of the legs), San Diego Instruments)], made in white ABS plastic, consists of two closed arms with walls 15 cm high and two open arms with no walls. Each mouse was placed randomly in one of the four arms and remained in the maze for 5 min while being recorded. The total time spent in open and closed arms and the number of times that the test mouse peaked out from the open arms were analyzed.

2.2.3. Light and dark box

A test mouse was placed in the dark side of a light-dark box [35 cm (W) x 17.5 cm (D) x 3 cm (H), Coulbourn Instruments] and allowed to explore free from interference for 5 min. The time elapsed before the mouse entered the light side as well as the total time spent in each side of the box was recorded and analyzed.

2.2.4. Rotarod test

A Rotamex-5 with mouse spindle (Columbus Instruments) was used to measure motor coordination. The test mouse was placed on the rotating rod accelerating from 5 to 100 rpm (accelerating 1 rpm every 5 s) during a 5 min session, and the time on the rod before falling was recorded. Each mouse was tested under the same parameters three times each day for three days. Data from all nine sessions was obtained and analyzed for each mouse.

2.2.5. Sociability and preference for social novelty

The test was carried out in a 45 cm × 45 cm × 37.5 cm (H) clear plastic chamber. Two small mesh cages (10 cm in diameter, 15 cm high) were placed at the opposite corners of two quadrants. The test mouse was allowed to explore the chamber freely for 10 min with the small empty mesh cages before starting test trials. For trial 1, a wild-type (C57BL/6) stranger male mouse was placed inside one of the mesh cages and the test mouse was allowed to explore the chamber freely for 5 min. For trial 2, a second wild-type stranger mouse (C57BL/6) was placed in the other mesh cage and the test mouse was allowed to explore freely for another 5 min. Total time of direct interaction as defined by sniffing and contact through the wired cage between the test and the stranger mouse or between the test mouse and the empty mesh cage were scored.

2.2.6. Dyadic male-male interaction in neutral field

The test was carried out in a 45 cm × 45 cm × 37.5 cm (H) clear plastic box that is unfamiliar to both test mouse and reference stranger mouse. A test mouse and a reference stranger male mouse of comparable age and C57BL/6 background were placed in the box that was separated by a divider. The mice were allowed to explore half of the box freely for 5 min. The divider was then removed, and the mice were allowed to interact for 10 min free from interference. Aggressive behavior (attacks and tail rattles) and nonaggressive social behavior (sniffing and following) of the test mouse were video-recorded and analyzed.

2.2.7. Self-grooming test

Each mouse was placed in a standard mouse cage that was clean and without bedding. The test mouse was given a 10 min habituation period. After that, they were scored for cumulative time spent in spontaneous grooming behaviors in all body regions, and number and length of self-grooming episodes during 10 min.

2.3. Immunoblot

Adult PC-specific *Grip1/2* knockout mice and control mice were sacrificed by overdoses of trifluoroethane. Cerebellum was quickly dissected on ice and snap frozen in liquid nitrogen. Then the tissues were homogenized with a polytron in lysis buffer (1% Nonidet P-40, 10% glycerol, 137 mM NaCl, 20 mM TrisHCl, pH 7,4) supplemented with a mixture of protease inhibitors (Roche) and phosphatase inhibitors (Roche). After incubation on ice for 30 min, the homogenized samples were centrifuged at 14,000 rpm for 10 min at 4 °C. The supernatants were used for Western blotting. Briefly, equal amounts of protein (20 μg) were separated by electrophoresis in Bis-Tris gels under reducing conditions and transferred onto PVDF membranes (Bio-rad) using standard procedures. The membranes were blocked in 5% nonfat milk for 1 h at RT and incubated overnight at 4 °C with rabbit anti-AKT (Cell Signaling), rabbit anti-phospho-AKT Thr308 (Cell Signaling), rabbit anti-Arc (AB_2313959, kindly provided by Dr. Paul Worley), mouse anti-GluR2 (NeuroLab), rabbit anti-pGluA2 pS880 (JH3068), mouse anti-Grip1 antibody (BD Biosciences), rabbit anti-Grip2 antibody (JH2986), rabbit anti-NR2A (JH6097), rabbit anti-NR2B (JH5523), rabbit anti-mTOR (Cell Signaling), rabbit anti-phospho-mTOR Ser2448 (Cell Signaling), rabbit anti-mGluR5 (Upstate), rabbit anti-P38 (Cell signaling), rabbit anti-phospho-P38 Thr180/Tyr182 (Cell signaling), rabbit anti-PICK1 (JH2906), or mouse anti- α tubulin (Santa Cruz) primary antibody. The blots were then incubated with the secondary antibody, goat anti-mouse or anti-rabbit IgG conjugated with horseradish peroxidase (1:5000–1:10,000); Perkin Elmer), for 1 h at RT. Signals were finally visualized using enhanced chemiluminescence (GE Healthcare), and the blots were exposed to X-ray film. Immunoblot signals were quantified using NIH-ImageJ. α-tubulin signal from each sample was used to normalize by protein levels. pAKT(T308) and p-P38 levels were normalized against total AKT and total P38, respectively.

2.4. Immunohistochemistry

Animals were sacrificed by overdose of trifluoroethane and immediately perfused first with PBS (phosphate-buffered saline) and then with 4% paraformaldehyde (dissolved in PBS, pH 7.4). Brains were carefully removed and postfixed for 4 h in 4% paraformaldehyde (dissolved in PBS, pH 7.4). Tissue was cryoprotected using 30% sucrose/PBS, pH 7.4. Brains were immersed in Tissue-Tek® O.C.T. compound (VWR) and frozen at −80 °C. Serial coronal sections (30 μm sections) were cut with a microtome. Free-floating sections were blocked with 4% goat serum/PBS plus 0.2% Triton X-100 and incubated with the primary antibody (anti-Grip1 antibody, BD Biosciences). Sections were sequentially incubated with biotin-conjugated anti-mouse (goat polyclonal; Jackson ImmunoResearch), ABC reagents (Vector Laboratories), and lastly SigmaFast DAB Peroxidase Substrate (Sigma) producing the dark brown reaction product in cells expressing Grip1.

2.5. Immunofluorescence

Mice were sacrificed by overdose of trifluoroethane and immediately perfused transcardially with PBS followed by 4% paraformaldehyde in PBS. Brains were removed and postfixed in the same fixative solution for 4 h. Tissue was then cryoprotected by immersion in a solution of 30% sucrose in PBS at 4 °C until it sank. Cerebellum was separated from the rest of the brain and immersed in Tissue-Tek® O.C.T. compound (VWR) and frozen at -80 °C. 30-μm-thick sagittal sections were cut using a sliding microtome. The slices were incubated in 10% Normal Goat Serum (NGS) with 0.1% Triton X-100 in PBS (blocking buffer) for 2 h. Primary antibodies (rabbit anti-AKT, Cell Signaling; rabbit anti-phospho-AKT Thr308, Cell Signaling; rabbit anti-mGluR5, Upstate; rabbit anti-P38, Cell signaling; or rabbit anti-phospho-P38 Thr180/Tyr182, Cell signaling) plus mouse anti-calbindin (Swant) were diluted in blocking buffer and slices were incubated overnight within them. After washing the antibodies with PBS, secondary fluorophore-conjugated antibodies (Alexa Fluor, Invitrogen) were added to the slices in blocking buffer and incubated for 4 h. Secondary antibodies were removed by washing with PBS. Slices were mounted onto Permafrost slides using Fluoromount-G Media (SouthernBiotech). Images were collected using a Zeiss LSM 510 Meta/NLO system (Carl Zeiss MicroImaging Group Inc.). Fluorescent intensities and cell body size and number were quantified using ImageJ software (NIH, National Institutes of Health). Cell body size and limits were determined based on calbindin signal.

2.6. Slice preparation and electrophysiology

Pairs of *Grip*-DKO and *Grip*-SKO mice at p24–32 were recorded at one animal per day in an interleaved manner with randomized sequence (some pairs started with DKO first and other pairs started with SKO first). Mice were anesthetized with the inhalation anesthetic isoflurane prior to decapitation. Sagittal slices of 250 μm from the cerebellar vermis were prepared in ice-cold, oxygenated *N*-methyl-D-glucamine (NMDG)-based cutting solution (135 mM NMDG, 1 mM KCl, 1.2 mM KH_2PO_4, 0.5 mM $CaCl_2$, 1.5 mM $MgCl_2$, 24.2 mM choline bicarbonate and 13 mM glucose). Slices were transferred to a chamber filled with artificial ACSF (124 mM NaCl, 2.5 mM KCl, 1.3 mM $MgCl_2$,

2.5 mM $CaCl_2$, 10 mM NaH_2PO_4, 26 mM $NaHCO_3$ and 20 mM glucose; pH 7.2; osmolality 300–305 mOsm) for a recovery incubation of 30 min at 32 °C followed by another recovery incubation for 1 h at room temperature before recording. For spontaneous AMPAR-mediated mEPSC recording, slices were perfused in artificial ACSF in the presence of 1 μM TTX and 5 μM gabazine at a flow rate of 2 ml/min. Whole cell recording pipettes (2–4 MΩ) were filled with internal solution I (88 mM Cs_2SO_4, 4 mM $MgSO_4$, 4 mM $CaCl_2$, 1.5 mM $MgCl_2$, 4 mM Na_2-ATP, 0.4 mM Na_3-GTP, 10 mM EGTA, HEPES 10 mM and 0.1 mM D600; pH 7.2, osmolality 290–295 mOsm). Cerebellar Purkinje neurons were patched and held at −70 mV holding potential and recording was performed at room temperature. Upon entering whole cell mode, we allowed 20 min for dialysis of the intracellular solution before collecting data. mEPSCs were detected with a template matching algorithm in Clampfit 10.2 software. A separate template was created for each recording by averaging around 30 of its most unambiguous mEPSCs as selected by eye. Averaged mEPSC amplitude and frequency were calculated from at least 400 events for each cell. SKO data were collected from 17 neurons/ 5 animals and DKO data were from 20 neurons/ 5 animals from 5 pairs of littermates. For cerebellar LTD recordings, slices were perfused in artificial ACSF in the presence of 5 μM gabazine. Whole cell recording pipettes (2–4 MΩ) were filled with internal solution II (135 mM Cs-methanesulfonate, 10 mM CsCl, 10 mM HEPES, 0.2 mM EGTA, 4 mM Na_2-ATP, and 0.4 mM Na-GTP (pH 7.2). Parallel fibers were stimulated in the molecular layer with paired pulses (100 ms interval) at a frequency of 0.1 Hz and 100 μs duration for test pulses). Stimulus strength was adjusted so that the first EPSC did not exceed 300 pA. To induce LTD, parallel fibers were stimulated with a train of five pulses at 100 Hz, which was accompanied by 100-ms-long depolarization of the Purkinje cell to 0 mV. A total of 30 trains were applied at 2 s intervals. Membrane currents were recorded with a MultiClamp 700B amplifier and digitized using a Digidata 1440A analog-to-digital board. Data acquisition were performed with pClamp 10.2 software and digitized at 10 kHz. All equipment and software are from Axon Instruments/Molecular Devices. Access resistance (Ra) was monitored throughout the recording and only cells with Ra < 15 mOhm with < 15% changes were included for quantification.

2.7. Statistical analysis

Recorded videos from mouse behavioral testing were analyzed by two investigators blinded to genotype. Data is presented as mean ± s.e.m. (standard error of the mean). Statistical details and statistical significance calculated using un-paired *t*-test, Mann Whitney test, two-way ANOVA or Factorial Repeated Measures ANOVA are indicated in the results or figure legends. Bonferroni *post hoc* test was used following two-way ANOVA; *, $p < .05$; **, $p < .01$.

3. Results

3.1. Generation of Purkinje Cell-specific Grip1/2 KO mice using an L7-Cre driver line

To investigate roles of Grip1/2-mediated AMPAR glutamate signaling disturbances in PCs with autism-associated phenotypes, we produced PC-specific *Grip1/2* KO mice by crossing *Grip2* conventional KO and *Grip1* conditional KO with L7-Cre mice to achieve PC-specific deletion of *Grip1 via* Let-7-Cre expression. Mice were genotyped using PCR-based methods for detection of WT, KO, flox and Cre bands (Fig. 1A). Western blot analyses using anti-Grip1 and anti-Grip2 antibodies reveled lack of Grip2 and minimal presence of Grip1 in cerebellum of L7-DKO mice (Fig. 1B). The low expression of Grip1 that remains in the cerebellum of L7-DKO mice could derive from a residual expression in some PCs or it could come from non-PC cell types that are present in the cerebellum (see also immunostaining of Grip1 on Fig. 1C). Immunohistochemical analyses showed that Grip1 is abundantly expressed in hippocampal pyramidal neurons (Fig. 1C, upper left panel) and cerebellar PCs (Fig. 1C, lower left panel) of L7-control mice. Although Grip1 expression is maintained in hippocampal pyramidal neurons (Fig. 1C, upper middle panel), there is an almost lack of expression observed in PCs from L7-DKO mice (Fig. 1C, lower middle panel). Complete lack of expression of Grip1 in hippocampus and cerebellum of Nestin-DKO mice (which have a deletion of *Grip1* in the whole brain) is shown for comparison (Fig. 1C, right panels). The number of PCs is reduced in postmortem brain tissues from autistic patients (reviewed by (Allen, 2005) and some mouse models of autism (Reith et al., 2012; Tsai et al., 2012). To determine whether Grip1/2 play a role in PCs survival, we performed calbindin (PC marker) staining on cerebellar slices from L7-DKO mice to analyze the Purkinje cell number and soma size. Mutant mice showed normal number and gross morphology of PCs in cerebellum at 6 months of age (cells/mm: L7-control, 34.6 ± 0.8; L7-DKO, 33.8 ± 0.9, $p = .518$, Student's *t*-test; soma size in μm^2: L7-control, 196.0 ± 5.6; L7-DKO, 202.4 ± 11.6, $p = .634$, Student's *t*-test; $n = 4$ per group) (Fig. 2A). In summary, these results demonstrate that L7-DKO mice have almost complete lack of Grip1/2 expression in the PCs of the cerebellum, with no effect on the number or gross morphology of these neurons.

3.2. PC-specific Grip1/2-KO mice show normal sociability and social interactions

Since neuron-specific *Grip1/2* KO mice (Nestin-DKO) showed altered social interactions (Mejias et al., 2011; Han et al., 2017), we conducted social behavioral tests including sociability, preference for social novelty, and dyadic male-male interaction in neutral field in L7-DKO mice. L7-DKO mice showed normal sociability (interaction with an empty cage in seconds: L7-control, 31.0 ± 3.0; L7-DKO, 45.2 ± 5.3; interaction with the cage with a stranger mouse in seconds: L7-control, 83.3 ± 9.1; L7-DKO, 81.0 ± 6.8; $n = 10–11$ per group, Genotype effect $p = .365$; Cage effect $p < .001$; Genotype-cage interaction $p = .213$; two-way ANOVA), preference for social novelty (interaction with the cage with a familiar mouse in seconds: L7-control, 43.6 ± 6.8; L7-DKO, 49.9 ± 9.1; interaction with the cage with a stranger mouse in seconds: L7-control, 66.6 ± 7.1; L7-DKO, 80.0 ± 7.2; n = 10–11 per group, Genotype effect $p = .201$; Cage effect $p = .001$, Genotype-cage interaction $p = .641$; two-way ANOVA) (Fig. 2B), and male-male social interactions in open arena (time sniffing (s): L7-control, 36.7 ± 8.8; L7-DKO, 36.4 ± 7.2, $p = .981$; time following: L7-control (s), 6.1 ± 2.1; L7-DKO, 6.1 ± 2.0; n = 10–11 per group, $p = .999$; Student's *t*-test) compared to age- and sex-matched L7-controls from the same strain background (Fig. 2C). We can conclude that lack of Grip1/2 expression in the PCs of the cerebellum does not have a major effect on social behaviors in mice.

3.3. PC-specific Grip1/2-KO mice show increased repetitive self-grooming behaviors

An increase in repetitive self-grooming in mice has been well established as an autism-related behavior in numerous mouse models of autism, and it has also be linked to other neuropsychiatric disorders (Silverman et al., 2010; Mehta et al., 2011; Peça et al., 2011). To assess this kind of behavior, we performed a spontaneous grooming test using adult male L7-DKO mice and their age- and sex-matched L7-controls of the same strain background. L7-DKO mice showed a significant increase in the cumulative time spent in repetitive grooming, and in the number of grooming episodes as compared to L7-control mice at 2–3 months of age (cumulative time grooming (s): L7-control, 25.37 ± 3.23; L7-DKO, 47.23 ± 9.63, $p = .038$; number of grooming episodes: L7-control, 8.55 ± 0.96; L7-DKO, 12.4 ± 1.35, $p = .029$; length of grooming episodes (s): L7-control, 3.17 ± 0.21; L7-DKO, 3.47 ± 0.49, $p = .555$; Student's *t*-test) (Fig. 3A, upper panel). Consistent with these findings, we detected a moderate increase in fine movements (small intermittent

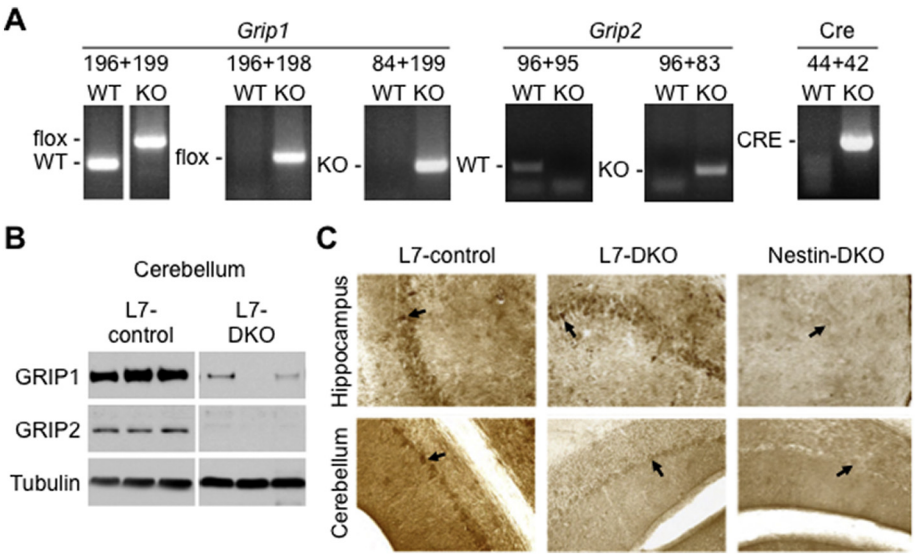

Fig. 1. Genotyping and Lack of Purkinje Cell-specific Expression of Grip1/2 in L7-DKO mice. (A) Representative genotyping performed by PCR using DNA extracted from tail of mice and showing WT, KO, flox and Cre bands. Different pairs of primers (196 + 199, 196 + 198, 84 + 199, 96 + 95, 96 + 83 and 44 + 42) were used for genotyping of each individual mouse. (B) Western blot analyses using antibodies anti-Grip1 and anti-Grip2 reveled lack of Grip2 and minimal presence of Grip1 in cerebellum of L7-DKO mice compared to control mice. L7-control and L7-DKO samples were run in the same gel and images come from the same membrane. (C) Hippocampus and cerebellum of L7-control, L7-DKO and Nestin-DKO mice were subjected to Grip1 immunostaining. Results showed that Grip1 is highly expressed in hippocampal pyramidal neurons (top left panel, signaled with an arrow) and cerebellar PCs of L7-control mice (bottom left panel, signaled with an arrow), and that L7-DKO mice have Grip1 protein in hippocampal pyramidal neurons (top middle panel, signaled with an arrow) but almost lack of Grip1 protein in cerebellar PCs (bottom middle panel, signaled with an arrow). Nestin-DKO mice, which have a deletion of *Grip1* in the whole brain, are shown for comparison (right panels).

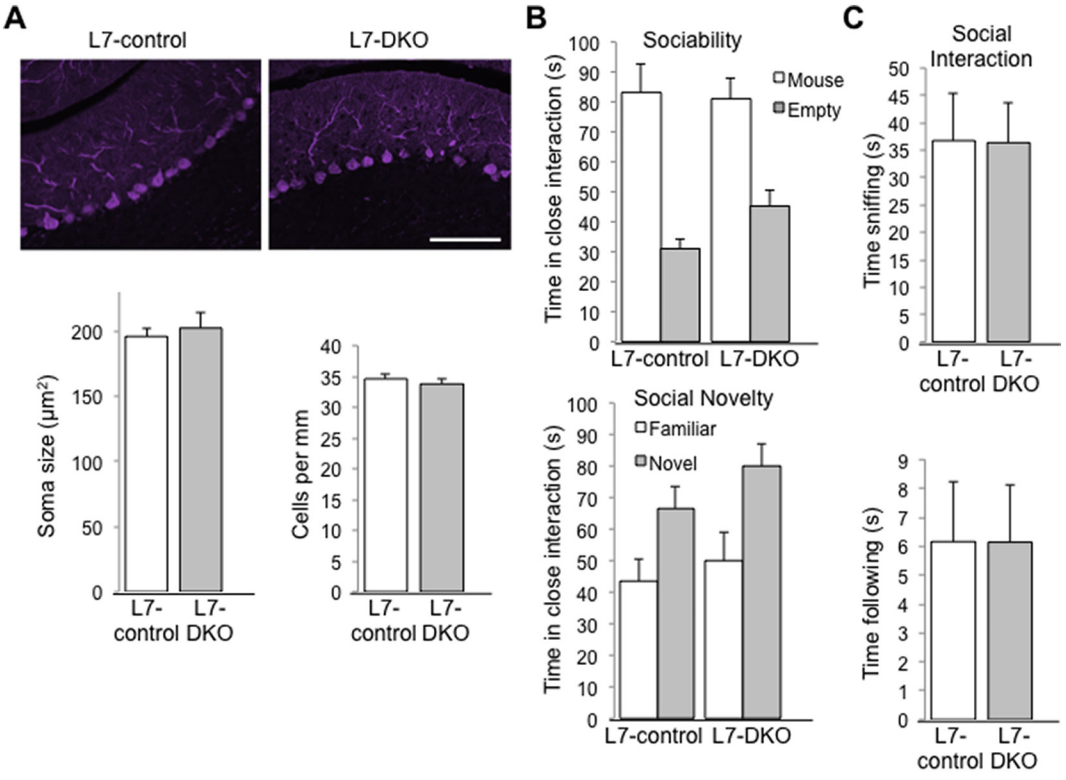

Fig. 2. Normal Number and Morphology of PCs, and Social Behaviors in PC-specific L7-DKO Mice. (A) Calbindin immunostaining of PCs in cerebellar sections from L7-control and L7-DKO mice (top panels); scale bar: 100 µm. There were no significant differences in soma size between L7-control and L7-DKO mice. Soma size was obtained by measurements of at least 150 PCs per animal with NIH-ImageJ software. Number of PCs per mm was similar between L7-control and L7-DKO mice. Counting was performed in 4–5 sections of the 6th cerebellar lobe of each animal with NIH-ImageJ software; Student's *t*-test; $n = 4$ mice per group. (B & C) Social behavior testing of L7-DKO mice showed normal sociability, social novelty and social interactions in mutant mice regarding L7-control animals; *b,* two-way ANOVA; *c,* Student's *t*-test; $n = 10$–11 mice per group.

bream breaks that occur when an animal stays in one place and moves in a stereotyped way in the open field chamber) of L7-DKO mice in the open field test (fine movements (number of beam breaks): L7-control, 338.8 ± 11.4; L7-DKO, 378.3 ± 13.8, $p = .038$; Student's *t*-test) (Fig. 3A, lower panel). To control for baseline behaviors that could potentially affect interpretations on test results for repetitive behaviors, we completed open field test, rotarod, dark and light box, and zero maze to assess motor activities and anxiety levels. PC-specific *Grip1/2* KO mice show normal ambulatory activities (central activity (number of beam breaks): L7-control, 3250.7 ± 316.1; L7-DKO, 2791.7 ± 302.1, $p = .309$; Student's *t*-test; peripheral activity (number of beam breaks): L7-control, 348.1 ± 34.4; L7-DKO, 380.3 ± 15.6,

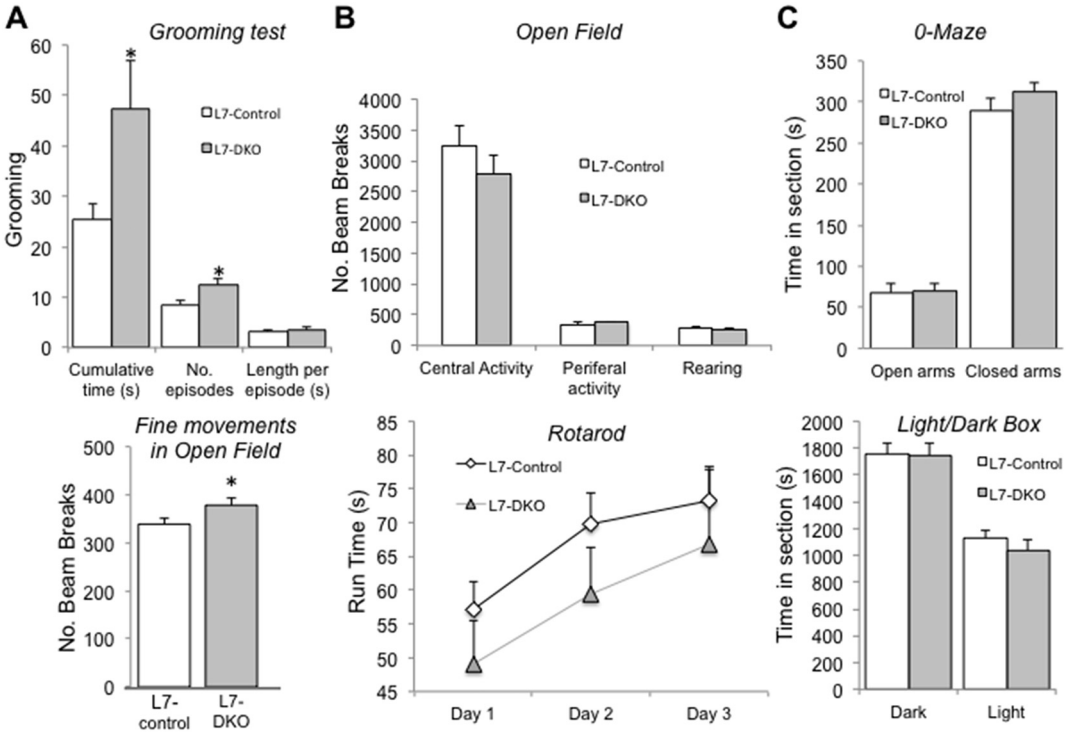

Fig. 3. Increased Repetitive Self-grooming but normal Ambulation and Anxiety in PC-specific L7-DKO Mice. (A) L7-DKO mice showed a significant increase in total time spent in grooming and in the number of grooming episodes as compared to L7-control mice (top panel). We detected a moderate increase in fine movements in open field in L7/DKO mice, further suggesting increase in repetitive behaviors (bottom panel); Student's *t*-test. (B) Open field and rotarod tests showed normal ambulatory activities and motor learning and balance in L7-DKO mice; upper B panel, Student's *t*-test; bottom B panel, Factorial Repeated Measures ANOVA. (C) O-maze and Light/Dark box tests indicated no differences in anxiety levels between L7-DKO and L7-control mice; Student's *t*-test; *$P < .05$; n = 10–11 mice per group.

$p = .515$; Student's *t*-test; rearing (number of beam breaks): L7-control, 283.7 ± 22.8; L7-DKO, 256.8 ± 34.9, $p = .518$; Student's t-test) (Fig. 3B, upper panel), motor learning and balance (Rotarod: run time (s): L7-control-day 1, 57.2 ± 4.1; L7-DKO-day 1, 49.1 ± 6.3; L7-control-day 2, 69.7 ± 4.7; L7-DKO-day 2, 59.5 ± 6.9; L7-control-day 3, 73.2 ± 5.2; L7-DKO-day 3, 66.9 ± 11.0; $p = .254$ Factorial Repeated Measures ANOVA) (Fig. 3B, lower panel), and anxiety levels (0-maze: time in open arms (s): L7-control, 67.9 ± 11.1; L7-DKO, 69.9 ± 9.0, $p = .889$; time in closed arms (s): L7-control, 289.2 ± 14.9; L7-DKO, 312.5 ± 11.4, $p = .236$; Student's *t*-test; Light/Dark box: time in dark section (s): L7-control, 1756.7 ± 77.9; L7-DKO, 1748.0 ± 85.1, $p = .941$; time in section with light (s): L7-control, 1124.5 ± 63.4; L7-DKO, 1040.4 ± 80.4, $p = .422$; Student's *t*-test) (Fig. 3C). Therefore, behavioral testing of L7-DKO mice identified an increase in repetitive self-grooming behaviors, but normal ambulatory activities and anxiety levels.

3.4. Loss of Grip1/2 expression blocks expression of mGluR-LTD at cerebellar PCs

mGluR-LTD at the parallel-fiber–Purkinje-cell synapses is a well-recognized mechanism for cerebellar function and information storage in cerebellum (Ito, 2001). Initial events of LTD induction are triggered by mGluR1 activation, Ca^{2+} influx and activation of AMPAR. These events induce Ca^{2+} release from the intracellular endoplasmic reticulum and activation of the protein kinase C (PKC) that results in enhanced AMPAR endocytosis. Unbinding of AMPAR subunit GluA2 from its binding to Grip1 and association with Arc (Activity-regulated cytoskeletal associated protein) are necessary for the internalization of AMPAR in cerebellar LTD (Eto et al., 2002; Luscher and Huber, 2010). Abnormal mGluR-LTD has been implicated in the pathogenesis of autism and intellectual disability(Luscher and Huber, 2010). Interestingly, recent studies have reported deregulation of mGluR-LTD in PCs in autism mouse models(Koekkoek et al., 2005; Baudouin et al., 2012; Piochon et al., 2014).

We showed previously that cerebellar mGluR-LTD was completely abolished in cultured PCs lacking Grip1/2 suggesting a key role for these proteins in the expression of mGluR-LTD (Takamiya et al., 2008) *in vitro*. To determine whether *Grip1/2* expression is crucial for mGluR-dependent function under conditions that preserve natural circuitry in cerebellum and to further study its involvement in repetitive grooming behaviors, we tested mGluR-LTD at the Parallel Fiber-PC synapses of neuron-specific *Grip1/2* KO mice using acute cerebellar slices. mGluR-LTD was induced in cerebellar slices by pairing a brief parallel fiber bursts with the depolarization of PCs. Since *Grip1*-mutations have been linked to autism (Mejias et al., 2011), we specifically assessed the role of *Grip1* expression by comparing electrophysiological data from neuron-specific *Grip1/2* double KO (*Grip*-DKO) with *Grip2* single KO (*Grip*-SKO) mice (Takamiya et al., 2008). The results showed a severely impaired mGluR-LTD in cerebellum of the *Grip*-DKO mice as compared to the *Grip*-SKO mice indicating that *Grip1* expression is crucial to mGluR-dependent plasticity in *ex vivo* slices (Fig. 4A, 30–35 min, SKO = 61.94 ± 5.85 and DKO = 89.66 ± 5.46%, $n = 6–7$ neurons from 4 to 6 mice per group; $p = .005$, Student's *t*-test). These studies detected no significant difference in the paired-pulse ratio suggesting that Grip1 do not affect presynaptic release and short-term plasticity (Fig. 4B, SKO = 1.57 ± 0.10 and DKO = 1.43 ± 0.06, n = 6–7 neurons from 4 to 6 mice per group; $p = .252$, Student's *t*-test). To assess whether Grip1 affects basal excitatory synaptic transmission, we studied spontaneous AMPAR-mediated miniature EPSC (AMPA-mEPSC) from PCs of *Grip*-DKO and *Grip*-SKO mice and detected no difference in either mEPSC amplitude (Fig. 4C, SKO: 16.39 ± 0.73 pA, $n = 17$; DKO: 16.19 ± 0.54, $n = 20$; $p = .99$, Mann-Whitney test) nor frequency (Fig. 4D, SKO: 3.85 ± 0.43 Hz, n = 17; DKO: 3.14 ± 0.24 Hz, n = 20; $p = .31$, Mann-Whitney test) indicating that synaptic transmission is intact in *Grip*-DKO mice at the resting state. Taken together, these

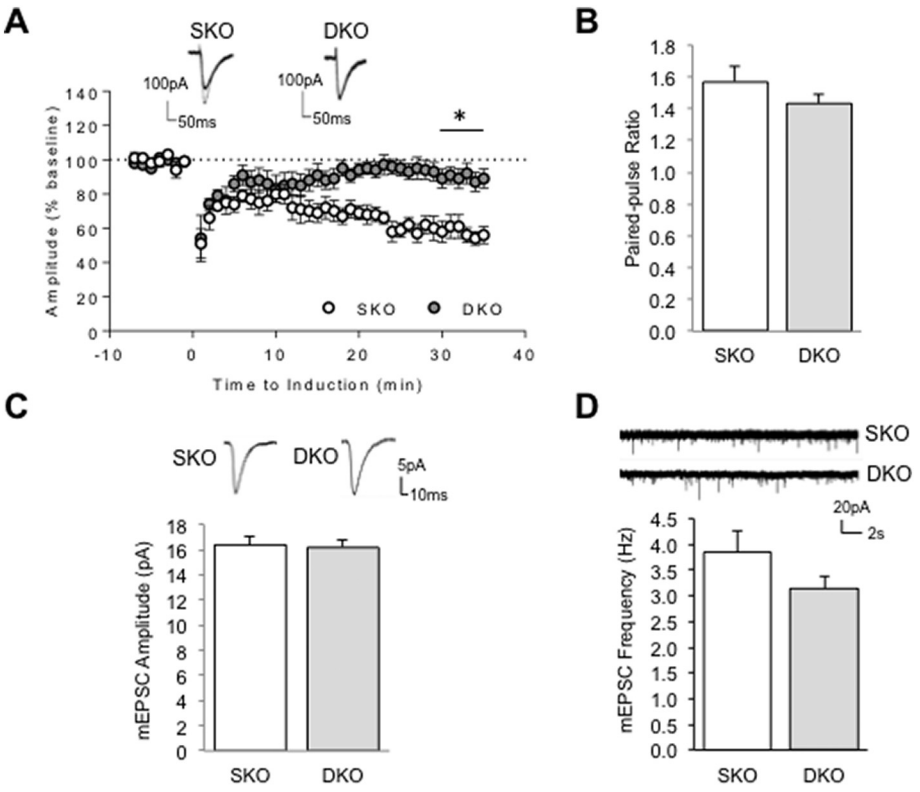

Fig. 4. Loss of mGluR-LTD at Parallel Fiber-PC synapses but Normal mEPSCs in Cerebellum of *Grip1/2* DKO Mice. (A) Cerebellar LTD was induced by stimulating parallel fibers in conjunction with a PC depolarization at $t = 0$ min. Evoked excitatory postsynaptic currents (EPSCs) were recorded from PCs in acute slices derived from one-month old *Grip2* single KO (SKO) or neuron-specific *Grip1/2* KO (*Grip*-DKO) animals. Depression was apparently observed in SKO (open circle) but not DKO (solid circle in grey). Example traces at 5-min before (thick line) and 25 min after (thin line) the LTD induction are overlaid on the top; Student's *t*-test; $n = 6$, neurons from 4 to 5 mice per group. (B) Parallel fibers were stimulated with a paired pulse with a 100-ms interval. Paired-pulse ratio was calculated as EPSC2/EPSC1. There is no difference noted between SKO and DKO; Student's *t*-test; n = 6 neurons from 4 to 5 mice per group. (C & D) Spontaneous AMPA receptor mediated miniature (mEPSC) were recorded in the presence of TTX and gabazine at −70 mV holding potential. AMPA mEPSC amplitude and frequency are comparable between PCs recorded from SKO and DKO mice. Individual mEPSCs and representative traces are showed on the top; Mann-Whitney test, $n = 17$ and 20 from 5 pair of mice; $^*P < .05$.

results demonstrate an activity-dependent regulation of Grip1 on AMPA receptor-medicated synaptic functions.

3.5. Enhanced expression of mGluR5 signaling proteins in cerebellum of L7-DKO mice

Cerebellar PC-mediated signaling and circuitry responsible for grooming behaviors in rodents are poorly understood. Disturbances in mTOR and mGluR signaling pathways have recently been implicated. We thus examined key mGluR-LTD and mTOR signaling proteins (P-AKT S473 and T308, Arc, GluA2, P-GluA2 S880, mGluR1, mGluR5, P-JNK, P-mTOR S2481 and S2448, NR2A, NR2B, P-P8, and PICK1) by immunoblot and found significant increased levels of Arc (OD in arbitrary units: L7-Control, 0.080 ± 0.03, L7-DKO, 0.338 ± 0.066; $p = .016$, Student's *t*-test), mGluR5 (OD in arbitrary units: L7-Control, 0.453 ± 0.019, L7-DKO, 0.566 ± 0.040; $p = .025$, Student's *t*-test), phosphorylated AKT/ Total AKT (T308) (OD in arbitrary units: L7-Control, 0.541 ± 0.038, L7-DKO, 0.822 ± 0.085; $p = .014$, Student's *t*-test), and phosphorylated P38/ Total P38 (OD in arbitrary units: L7-Control, 1.182 ± 0.221, L7-DKO, 2.597 ± 0.324; $p = .018$, Student's *t*-test) in cerebellum of PC-specific *Grip1/2* KO mice (Fig. 5). Levels of phosphorylated P38, total P38, phosphorylated ATK, and total AKT were also normalized by the loading control (Tubulin) and we only found a statistically significant increase for phospho-P38 but no other significant changes for the rest of proteins tested (data not shown). These results demonstrate a significant increase in mGluR5 and mTOR signaling in cerebellum of PC-specific *Grip1/2* KO mice.

4. Discussion

Structural and functional anomalies in cerebellum and PCs have been found in patients and mouse models of autism (Becker and Stoodley, 2013). PC-specific knockout mice of autism-associated genes including *Fmr1*, *Tsc1*, and *Shank2* showed variable disturbances in motor and/or social behaviors, which support an important role of cerebellar PCs in autism pathogenesis (Koekkoek et al., 2005; Tsai et al., 2012; Peter et al., 2016). Disrupted cerebellar functions have also been implicated in the pathogenesis of Tourette Syndrome, tic phenotypes in obsessive-compulsive disorder, and compulsive skin-picking (Tobe et al., 2010; Wabnegger and Schienle, 2019). However, PCs-specific signaling mechanisms in these disorders have not been fully characterized.

Abnormally increased repetitive self-grooming in mice has been used to model pathological repetitive behaviors in several neuropsychiatric disorders including autism spectrum disorders (Feusner et al., 2009; Won et al., 2012; Sungur et al., 2014; Kalueff et al., 2016; Wang et al., 2017). Our data show that lack of Grip1/2 expression without apparent loss in PCs results in increased self-grooming behaviors in mice, which further support a critical role of cerebellum and more specifically PCs on regulating repetitive behaviors in mice. While loss of PC has been extensively reported in post-mortem studies of patients with autism, our data suggest that disturbances in signaling pathways contributing to autism phenotypes occur without apparent cell death. This observation is supported by previous studies on PC-specific *Tsc1* knockout mice that display abnormal vocalizations and impaired motor learning prior to detectable loss of PCs (Tsai et al., 2012). Thus, characterizing disrupted signaling pathways in PCs is critically important to elucidate pathogenesis of cerebellar phenotypes in autism spectrum disorders.

Autism-associated mutations at *Grip1*-PDZ domains 4–6 have been described and neuron-specific *Grip1/2* KO mice show altered social interactions but normal self-grooming behaviors (Mejias et al., 2011). In contrast, PC-specific *Grip1/2* KO mice show normal social interactions but increased self-grooming suggesting that the effect of Grip1/2-mediated AMPAR signaling on social behaviors is not cerebellum-dependent. Differences in behavioral phenotypes between conventional KO and Purkinje neuron-specific KO mice have been observed previously. For example, *Shank2* conventional KO mice carrying a human autism microdeletion ($Shank2^{-/-;\ del\text{-}ex15\text{–}16}$) were found to have autism-like behaviors including reduced social interaction, reduced social communication by ultrasonic vocalizations, and repetitive jumping (Won et al., 2012). *Shank2*-mutant mice carrying this identical

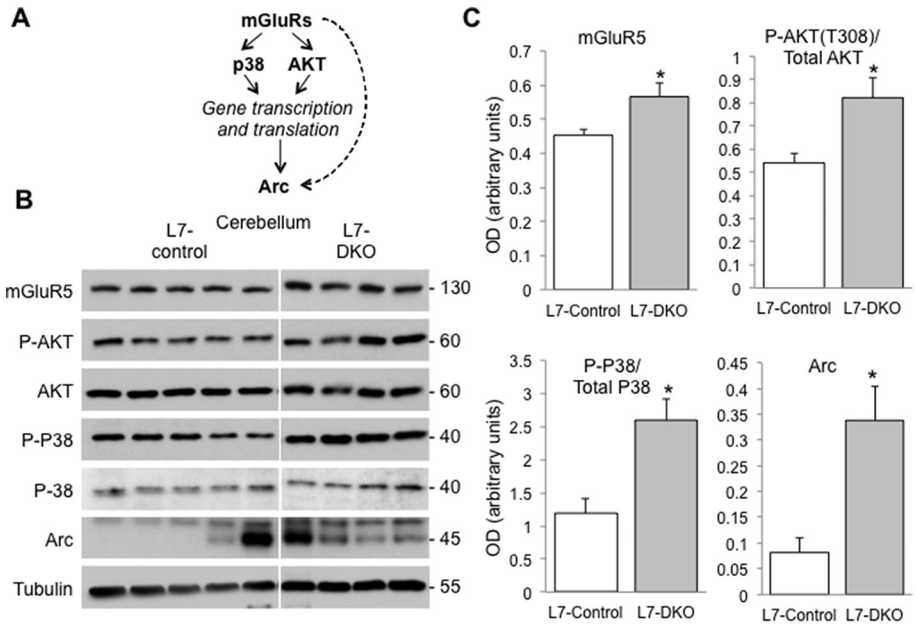

Fig. 5. Over-expression of mGluR5 and mGluR-LTD Signaling Proteins in Cerebellum of PC-specific L7-DKO mice. (A) A schematic diagram of mGluR-LTD signaling pathway. Activation on mGluRs by glutamate induces phosphorylation of P38 and AKT among other proteins, and a subsequently increase in gene transcription and protein translation. One of the targets that increments its expression is Arc, a scaffolding protein that interacts with microtubules and AMPAR subunits. Arc can also be activated directly by mGluRs, but the specific mechanisms are unknown. (B) Western blot analyses in cerebellum of L7-DKO and L7-Control mice showed an increase in the levels of mGluR5, P-AKT (T308)/Total AKT, P-P38/Total P38 and Arc; MW of the bands detected is shown in kDa. (C) Densitometric quantitation of the blots using NIH-ImageJ. L7-control and L7-DKO samples were run in the same gel and images come from the same membrane. Tubulin signal was used as loading control; Student's *t*-test; *P < .05; n = 4–5 mice per group.

mutation in Purkinje neurons (*Shank2* $^{\text{del-ex15–16–L7-Cre}}$) showed impaired motor coordination, learning, and repetitive behaviors but without social interaction deficits (Ha et al., 2016). These differences are expected because multiple brain regions and neural circuitries including cortico-basal ganglia-thalamic circuits, limbic system, prefrontal cortex and cerebellum are known to regulate social and repetitive behaviors (Nickl-Jockschat et al., 2012). Understanding the mechanisms responsible for these differences could help to define specific roles of brain regions and circuitries in the regulation of autism-associated social behaviors and repetitive phenotypes. Our data support that Grip1/2 expression in PCs plays an important role in modulating repetitive self-grooming behaviors while Grip1/2 expression in neurons of other regions including limbic system play a large role in modulating social behaviors.

mGluR-LTD at parallel-fiber–Purkinje-cell synapses is a well-recognized cellular model of cerebellar information storage (Ito, 2001). Initial postsynaptic events necessary for cerebellar LTD include mGluR1 and AMPAR activation, and an influx of calcium that converge in the activation of protein kinase C (PKC). mGluR-LTD activation is expressed in part through a change in internalization and a loss of postsynaptic surface AMPARs depending on rapid endocytosis and/or reduced recycling of GluA2-containing AMPARs (Linden and Connor, 1991; Wang and Linden, 2000; Waung et al., 2008). Unbinding of AMPA receptor subunit GluA2 with Grip1 and association with Arc and PICK1 appear to be necessary for the internalization of AMPAR in cerebellar LTD (Eto et al., 2002; Luscher and Huber, 2010). Our previous works showed that lack of Grip1/2 expression results in severely impaired mGluR-LTD at PCs in culture and this effect is mediated primarily by Grip1 (Takamiya et al., 2008). Our current studies identified a severely impaired mGluR-LTD in cerebellum of Grip1/2-DKO mice compared to that of Grip2-SKO mice using *ex vivo* slices (Fig. 4). Together, these finding provides supports to the hypothesis that Grip1 expression plays a major role in mGluR-dependent plasticity in cerebellum. We propose that loss of Grip1/2 impedes an effective recycling of AMPARs in postsynaptic surface, which contributes to a lack of mGluR-LTD at the parallel-fiber–Purkinje-cell synapses.

Results from our current studies do not establish that changes in mGluR-LTD are directly causal to enhanced repetitive grooming in the mutant mice. Interestingly, we identified an increased expression of mGluR5 signaling proteins including mGluR5 and Arc, and enhanced phosphorylation of p38 and AKT in cerebellar tissues of these mice. Activation of mGluR5 signaling is known to induce local translation of Arc, which plays a critical role in initiation of mGluR-LTD by triggering endocytosis of postsynaptic AMPARs (Waung et al., 2008). We propose that activation of mGluR5 signaling functions as a compensatory mechanism to AMPARs recycling defects caused by a loss of PC-specific Grip1/2 expression.

Dysregulations of mGluR-LTD have been found in several animal models of neurodevelopmental disorders including intellectual disability and autism (Wilkerson et al., 2018). An abnormally enhanced mGluR5 signaling with increased expression of mGluR-LTD with elevated levels of Arc were detected in *fmr1*-KO mice (Huber et al., 2002; Koekkoek et al., 2005). Consistent with this mechanism, several mGluR5 antagonists such as MPEP were tested in mouse models of FXS and autism and found to ameliorate core behavioral phenotypes including social deficits and enhanced repetitive behaviors (Nakamoto et al., 2007; Silverman et al., 2010; Mehta et al., 2011). Interestingly, an reduced mGluR-LTD has been found in hippocampus of $Tsc^{+/-}$ mice modeling Tuberous Sclerosis 2 (Auerbach et al., 2011) and *Ube3A*-deficent mice modeling Angelman syndrome (Pignatelli et al., 2014). Our current data from studying PC-specific *Grip1/2* knockout mice suggest that altered AMPAR trafficking at Purkinje synapses with a compensatory activation of mGluR5 signaling in cerebellum contribute to enhanced repetitive self-grooming in mice. Taken together, results from these studies support that optimal levels of mGluR5 signaling and mGluR-LTD are crucial for a normal development of cognitive functions and behaviors (Wilkerson et al., 2018).

Funding

This work was supported in part by grants from Simons Foundation for Autism Research Initiative (SFARI) (#0206683), U.S.A. and National Institute of Health (NIH) (MH112808), U.S.A. to R.H. and T.W. RM was supported in part by a postdoctoral fellowship from the University of Seville (V PPIT-US), Spain and an National Institute of Health (NIH) (NS085358), U.S.A.

Declaration of Competing Interest

The authors declare no competing financial interests.

Acknowledgements

The authors thank Dr. Paul Worley of Johns Hopkins University for invaluable discussions and for providing reagents to this work. We dedicate this manuscript to Yifan Zhao, a recently deceased graduate student who helped analyzing rodent behavioral tests included in this work.

References

Adamczyk, A., Mejias, R., Takamiya, K., Yocum, J., Krasnova, N., Calderon, J., Cadet, J., Huganir, R., Pletnikov, M., Wang, T., 2012. GluA3-deficiency in mice is associated with increased social and aggressive behavior and elevated dopamine in striatum. Behav. Brain Res. 229, 265–275.

Allen, G., 2005. The cerebellum in autism. Clin. Neuropsychiatry 2, 321–337.

Aparks, B., Griedman, S., Shaw, D., Aylward, E., Echelard, D., Artru, A., Maravilla, K., Giedd, J., Munson, H., Dawson, G., Dager, S., 2002. Brain structural abnormalities in young children with autism spectrum disorder. Neurology 59, 184–192.

Araghi-Niknam, M., Fatemi, S., 2003. Levels of Bcl-2 and P53 are altered in superior frontal and cerebellar cortices of autistic subjects. Cell. Mol. Neurobiol. (6), 945–952.

Auerbach, B., Osterweil, E., Bear, M., 2011. Mutations causing syndromic autism define an axis of synaptic pathophysiology. Nature 480, 63–68.

Ayhan, Y., Abazyan, B., Nomura, J., Kim, R., Ladenheim, B., Krasnova, I.N., Sawa, A., Margolis, R.L., Cadet, J.L., Mori, S., Vogel, M.W., Ross, C.A., Pletnikov, M.V., 2011. Differential effects of prenatal and postnatal expressions of mutant human DISC1 on neurobehavioral phenotypes in transgenic mice: evidence for neurodevelopmental origin of major psychiatric disorders. Mol. Psychiatry 16, 293–306.

Baudouin, S., Gaudias, J., Gerharz, S., Hatstatt, L., Zhou, K., Punnakkal, P., Tanaka, K., Spooren, W., Hen, R., De Zeeuw, C., Vogt, K., Scheiffele, P., 2012. Shared synaptic pathophysiology in syndromic and nonsyndromic rodent models of autism. Science 338, 128–132.

Bauman, M., Kemper, T., 1985. Histoanatomic observations of the brain in early infantile autism. Neurology 35, 866–874.

Becker, E., Stoodley, C., 2013. Autism spectrum disorder and the cerebellum. International Rev Neurobiol 113, 1–34.

Carper, R., Courchesne, E., 2000. Inverse correlation between frontal lobe and cerebellum sizes in chidren with autism. Brain 123, 836–844.

Courchesne, E., Karns, C., Davis, H., Ziccardi, R., Carper, R., Tigue, Z., Chisum, H., Moses, P., Pierce, K., Lord, C., Lincoln, A., Pizzo, S., Schreibman, L., Haas, R., Akshoomoff, N., Courchesne, R., 2001. Unusual brain growth patterns in early life in patients with autistic disorder: an MRI study. Neurology 57, 245–254.

Eto, M., Bock, R., Brautigan, D., Linden, D., 2002. Cerebellar long-term synaptic depression requires PKC-mediated activation of CPI-17, a myosin/moesin phosphatase inhibitor. Neuron 36, 1145–1158.

Fatemi, S., Halt, A., Stary, J., Kanodia, R., Schulz, S., Realmuto, G., 2002. Glutamic acid decarboxylase 65 and 67 kDa proteins are reduced in autistic parietal and cerebellar cortices. Biol. Psychiatry 52, 805–810.

Feusner, J., Hembacher, E., Phillips, K., 2009. The mouse who Couldn't stop washing: pathologic grooming in animals and humans. CNS Spectr 14, 503–513.

Gottwald, B., Wilde, B., Mihajlovic, Z., Mehdorn, H., 2004. Evidence for distinct cognitive deficits after focal cerebellar lesions. J. Neurol. Neurosurg. Psychiatry 75, 1524–11531.

Ha, S., Lee, D., Cho, Y., Chung, C., Yoo, Y., Kim, J., Lee, J., Kim, W., Kim, H., Bae, Y., Tanaka-Yamamoto, K., Kim, E., 2016. Cerebellar Shank2 regulates excitatory synapse density, motor coordination, and specific repetitive and anxiety-like behaviors. J. Neurosci. 36, 12129.

Han, M., Mejias, R., Chiu, S., Rose, R., Adamczyk, A., Huganir, H., Wang, T., 2017. Mice lacking GRIP1/2 show increased social interactions and enhancedphosphorylation at GluA2-S880. Behav. Brain Res. 321, 176–184.

Herbert, M., Ziegler, D., Deutsch, C., O'Brien, L., Lange, N., Kennedy, D., Harris, G., Caviness, V., 2003. Dissociations of cerebral cortex, subcortical and cerebral white matter volumes in autistic boys. Brain 126, 1182–1192.

Huber, K., Gallagher, S., Warren, S., Bear, M., 2002. Altered synaptic plasticity in a mouse model of fragile X mental retardation. Proc. Natl. Acad. Sci. U. S. A. 99, 7746–7750.

Ito, M., 2001. Cerebellar long-term depression: characterization, singal transduction, and functional roles. Phsiol Rev 81, 1143–1195.

Kalueff, A., Stewart, A., Song, C., Berridge, K., Graybiel, A., Fentress, J., 2016. Neurobiology of rodent self-grooming and its value for translational neuroscience. Nat. Rev. Neurosci. 17, 45–59.

Kaufmann, W., Cooper, K., Mostofsky, S., Capone, G., Kates, W., Newschaffer, C., Bukelis, I., Stump, M., Jann, A., Lanham, D., 2003. Specificity of cerebellar vermian abnormalities in autism: a quantitative magnetic resonance imaging study. J Child Neuro 18, 463–470.

Koekkoek, S., Yamaguchi, K., Milojkovic, B., Dortland, B., Ruigrok, T., Maex, R., De Graaf, W., Smit, A., VanderWerf, F., Bakker, C., Willemsen, R., Ikeda, T., Kakizawa, S., Onodera, K., Nelson, D., Mientjes, E., Joosten, M., De Schutter, E., Oostra, B., Ito, M., De Zeeuw, C., 2005. Deletion of FMR1 in Purkinje cells enhances parallel fiber LTD, enlarges spines, and attenuates cerebellar eyelid conditioning in Fragile X syndrome. Neuron 47, 339–352.

Laurence, J., Fatemi, S., 2005. Glial fibrillary acidic protein is elevated in superior frontal, parietal and cerebellar cortices of autistic subjects. Cerebellum 4, 206–210.

Levisohn, L., Cronin-Golomb, A., Schmahmann, J., 2000. Neuropsychological consequences of cerebellar tumour resection in children. Cerebellar cognitive affective syndrome in a paediatric population. Brain 123, 1041–1050.

Levitt, J., Blanton, R., Capetillo-Cunliffe, L., Guthrie, D., Toga, A., McCracken, J., 1999. Cerebellar vermis lobules VIII-X in autism. Prog Neuropsychopharma Biol Psychiatry 23, 625–633.

Linden, D., Connor, J., 1991. Participation of postsynaptic PKC in cerebellar long-term depression in culture. Science 254, 1656–1659.

Luscher, C., Huber, K., 2010. Group 1 mGluR-dependent synaptic long-term depression: mechanisms and implications for circuitry and disease. Neuron 65, 445–459.

Mao, L., Takamiya, K., Thomas, G., Lin, D.T., Huganir, R.L., 2010. GRIP1 and 2 regulate activity-dependent AMPA receptor recycling via exocyst complex interactions. Proc. Natl. Acad. Sci. U. S. A. 107, 19038–19043.

Martin, L., Goldowitz, D., Mittleman, G., 2010. Repetitive behavior and elevated activity in mice with Purkinje cell loss: a model for understanding the role of cerebellar pathology in autism. Eur. J. Neurosci. 31, 544–555.

McNaughton, C.H., Moon, J., Strawderman, M.S., Maclean, K.N., Evans, J., Strupp, B.J., 2008. Evidence for social anxiety and impaired social cognition in a mouse model of fragile X syndrome. Behav. Neurosci. 122, 293–300.

Mehta, M., Ganal, M., Siegel, S., 2011. mGluR5-Antagonist mediated reversal of elevated stereotyped, repetitive behaviors in the VPA model of autis. PLoS One 6, e26077.

Mejias, R., Adamczyk, A., Anggono, V., Niranjan, T., Thomas, G., Sharma, K., Skinner, C., Schwartz, C., Stevenson, R., Fallin, M., Kaufmann, W., Pletnikov, M., Valle, D., Huganir, R., Wang, T., 2011. Gain-of-function glutamate receptor interacting protein 1 variants alter GluA2 recycling and surface distribution in patients with autism. Proc. Natl. Acad. Sci. U. S. A. 108, 4920–4925.

Nakamoto, M., Nalavadi, V., Epstein, M.P., Narayanan, U., Bassell, G.J., Warren, S.T., 2007. Fragile X mental retardation protein deficiency leads to excessive mGluR5-dependent internalization of AMPA receptors. Proc. Natl. Acad. Sci. U. S. A. 104, 15537–15542.

Nickl-Jockschat, T., Habel, U., Michel, T., Manning, J., Laird, A., Fox, P., Schneider, F., Eickhoff, S., 2012. Brain structure anomalies in autism spectrum disorder—a meta-analysis of VBM studies using anatomic likelihood estimation. Hum. Brain Mapp. 33, 1470–1489.

Palmen, S., Hulshoff Pol, H., Kemner, C., Schnack, H., Hanssen, H., Kahn, R., van Engeland, H., 2004. Large brains in medication naive high-functioning subjects with pervasive developmental disorder. J Aut Dev Dis 34, 603–613.

Peça, J., Feliciano, C., Ting, J., Wang, W., Wells, M., Venkatraman, T., Lascola, C., Fu, Z., Feng, G., 2011. Shank3 mutant mice display autistic-like behaviours and striatal dysfunction. Nature 472, 437–442.

Peter, S., Ten Brinke, M., Stedehouder, J., Reinelt, C., Wu, B., Zhou, H., Zhou, K., Boele, H., Kushner, S., Lee, M., Schmeisser, M., Boeckers, T., Schonewille, M., Hoebeek, F., De Zeeuw, C., 2016. Dysfunctional cerebellar Purkinje cells contribute to autism-like behaviour in Shank2-deficient mice. Nat. Commun. 7, 12627.

Pietropaolo, S., Guilleminot, A., Martin, B., D'Amato, F.R., Crusio, W.E., 2011. Genetic-background modulation of core and variable autistic-like symptoms in Fmr1 knock-out mice. PLoS One 6, e17073.

Pignatelli, M., Piccinin, S., Molinaro, G., Di Menna, L., Riozzi, B., Cannella, M., Motolese, M., Vetere, G., Catania, M., Battaglia, G., Nicoletti, F., Nisticò, R., Bruno, V., 2014. Changes in mGlu5 receptor-dependent synaptic plasticity and coupling to homer proteins in the hippocampus of Ube3A hemizygous mice modeling angelman syndrome. J. Neurosci. 34, 4558–4566.

Piochon, C., Kloth, A., Grasselli, G., Titley, H., Nakayama, H., Hashimoto, K., Wan, V., Simmons, D., Eissa, T., Nakatani, J., Cherskov, A., Miyazaki, T., Watanabe, M., Takumi, T., Kano, M., Wang, S., Hansel, C., 2014. Cerebellar plasticity and motor learning deficits in a copy-number variation mouse model of autism. Nat. Commun. 5, 5586.

Pletnikov, M.V., Ayhan, Y., Nikolskaia, O., Xu, Y., Ovanesov, M.V., Huang, H., Mori, S., Moran, T.H., Ross, C.A., 2008. Inducible expression of mutant human DISC1 in mice is associated with brain and behavioral abnormalities reminiscent of schizophrenia. Mol. Psychiatry 13, 173–186, 115.

Purcell, A., Jeon, O., Zimmerman, A., Blue, M., Pevsner, J., 2001. Postmortem brain abnormalities of the glutamate neurotransmitter system in autism. Neurology 57, 1618–1628.

Reith, R., McKenna, J., Wu, H., Hashmi, S., Cho, S., Dash, P., Gambello, M., 2012. Loss of Tsc2 in Purkinje cells is associated with autistic-like behavior in a mouse model of tuberous sclerosis complex. Neurobiol. Dis. 51, 93–103.

Ritvo, E., Freeman, B., Scheibel, A., Duong, T., Robinson, H., Guthrie, D., Ritvo, A., 1986. Lower Purkinje cell counts in the cerebella of four autistic subjects: initial findings of the UCLA–NSAC autopsy research project. Am. J. Psychiatry 143, 862–866.

Riva, D., Giorgi, D., 2000. The cerebellum contributes to higher functions during development: evidence from a series of children surgically treated fro posterior fossa tumours. Brain 123, 1051–1061.

Schmahmann, J., Sherman, J., 1998. The cerebellar cognitive affective syndrome. Brain 121, 561–579.

Silverman, J., Tolu, S., Barkan, C., Crawley, J., 2010. Repetitive self-grooming behavior in the BTBR mouse model of autism is blocked by the mGluR5 antagonist MEPE. Neuropsychopharmacology 35, 976–989.

Sungur, A., Vörckel, K., Schwarting, R., Wöhr, M., 2014. Repetitive behaviors in the Shank1 knockout mouse model for autism spectrum disorder: developmental aspects and effects of social context. J. Neurosci. Methods 234, 92–100.

Takamiya, K., Mao, L., Huganir, R.L., Linden, D.J., 2008. The glutamate receptor-interacting protein family of GluR2-binding proteins is required for long-term synaptic depression expression in cerebellar Purkinje cells. J. Neurosci. 28, 5752–5755.

Tobe, R., Bansal, R., Xu, D., Hao, X., Liu, J., Sanchez, J., Peterson, B., 2010. Cerebellar morphology in Tourette syndrome and obsessive-compulsive disorder. Ann. Neurol. 67, 479–487.

Tsai, P., Hull, C., Chu, Y., Greene-Colozzi, E., Sadowski, A., Leech, J., Steinberg, J.,

Crawley, J., Regehr, W., Sahin, M., 2012. Autistic-like behaviour and cerebellar dysfunction in Purkinje cell Tsc1 mutant mice. Nature 488, 647–651.
Wabnegger, A., Schienle, A., 2019. The role of the cerebellum in skin-picking disorder. Cerebellum 18, 91–98.
Wang, Y., Linden, D., 2000. Expressiom of cerebellar long-term depression requires postsynaptic clathrin-mediated endocyosis. Neuron 25, 635–647.
Wang, W., Li, C., Chen, Q., van der Goes, M., Hawrot, J., Yao, A., Gao, X., Lu, C., Zang, Y., Zhang, Q., Lyman, K., Wang, D., Guo, B., Wu, S., Gerfen, C., Fu, Z., Feng, G., 2017. Striatopallidal dysfunction underlies repetitive behavior in Shank3-deficient model of autism. J. Clin. Invest. 127, 1978–1990.
Waung, M., Pfeiffer, B., Nosyreva, E., Ronesi, J., Huber, K., 2008. Rapid translation of Arc/Arg3.1 selectively mediates mGluR-dependent LTD through persistent increases in AMPAR endocytosis rate. Neuron 59, 84–97.
Wilkerson, J., Albanesi, J., Huber, K., 2018. Roles for Arc in metabotropic glutamate receptor-dependent LTD and synapse elimination: implications in health and disease. Seminars in Cell Develop Biol 77, 51–62.
Won, H., Lee, H., Gee, H., Mah, W., Kim, J., Lee, J., et al., 2012. Autistic-like social behaviour in Shank2-mutant mice improved by restoring NMDA receptor function. Nature 486, 261–265.